Bed Shear-stresses Under Combined Waves and Currents on Smooth and Rough Beds

Produced within Defra project FD1905 (EstProc)

R.L. Soulsby and S. Clarke

Report TR 137
Rev 1.0
August 2005

HR Wallingford

Estuary Processes Research Project/Defra project FD1905
Bed Shear-stresses Under Combined Waves and Currents on Smooth and Rough Beds

HR Wallingford

Document Information

Project	Estuary Processes Research Project (Est Proc)/Defra project FD1905
Report title	Bed Shear-stresses Under Combined Waves and Currents on Smooth and Rough Beds
Client	Defra/Environment Agency Flood and Coastal Defence R&D Programme
Client Representative	Dr Jonathan Rogers, Mouchel
Project No.	CBS0022
Report No.	TR 137
Doc. ref.	TR137 smooth and rough beds rev 1-0.doc
Project Manager	RJS Whitehouse
Project Sponsor	RL Soulsby

Document History
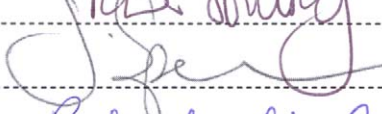
Date	Release	Prepared	Approved	Authorised	Notes
18/08/05	1.0	R Soulsby	J Spearman	R Whitehouse	Minimum value of T_1 set to 12. Values of a_r and a_s both set to 0.24. Various clarifications in text.

Prepared

Approved

Authorised

© Crown Copyright (Defra)   August 2005

Summary

Bed Shear-stresses Under Combined Waves and Currents on Smooth and Rough Beds

R L Soulsby and S Clarke

Report TR 137
August 2005

Calculations and numerical modelling of the erosion, transport and deposition of sediments in estuaries and coastal areas rely heavily on expressions that contain the bed shear-stress, representing the friction exerted by the flowing water on the bed. In general the bed shear-stress is generated by the combined effects of waves and currents, whose turbulent boundary layers interact non-linearly. The flow is usually considered to be hydrodynamically rough turbulent for sand and gravel beds, and hydrodynamically smooth turbulent for freshly-deposited mud beds. Most existing theories and models for the wave-current-interaction have considered only the rough bed case, and they have generally been too complicated and computer-intensive to be usable in whole-estuary (or coastal) models.

This report produced within Defra project FD1905 (Est Proc) describes the development and testing of a new method of calculating the mean, maximum and root-mean-square bed shear-stresses due to combined waves and currents. The method caters for rough turbulent and smooth turbulent (and also laminar) flows, with the greatest emphasis on the less well-researched smooth turbulent case. Tests of the new method against published data for smooth flows gave better agreement than existing methods. The new method is also simpler, being expressed as explicit algebraic equations that are computationally fast. A detailed algorithm giving the "recipe" to implement the method is given in an appendix.

Acknowledgements

Notation

$A = U_w T / (2\pi)$	orbital amplitude of wave motion at the bed
A_1, A_2, a, b	terms in solution for u_{*m}
a_r, a_s	coefficients prescribing δ for rough, smooth flow
C_D	drag coefficient applicable to depth-averaged current
C_{Dm}, C_{Dmax}	mean, maximum value of drag coefficient during wave cycle
cos	cosine
d_{50}	median grain diameter
e	$2 \cdot 718281828$
f_w	wave friction factor
f_{wr}	rough bed wave friction factor
f_{ws}	smooth bed wave friction factor
g	acceleration due to gravity $= 9 \cdot 81 ms^{-2}$
h	water depth
ln	natural logarithm (to base e)
n	general power
$Re_c = \overline{U}h / \nu$	current Reynolds number
$Re_{c,cr}, Re_{w,cr}$	critical value of Re_c, Re_w at transition to turbulence
$Re_w = \dfrac{U_w A}{\nu}$	wave Reynolds number
sin	sine
T	period of water wave
T_1, T_2, T_3	terms in solution for C_{Dm} and C_{Dmax}
t	time
U	horizontal component of water velocity
$\overline{U}$	depth-averaged current speed
$u_* = (\tau_0 / \rho)^{1/2}$	friction velocity
$u_{*e} = (\tau_e/\rho)^{1/2}$	effective friction velocity
$u_{*m} = (\tau_m / \rho)^{1/2}$	mean friction velocity
$u_{*max} = (\tau_{max} / \rho)^{1/2}$	maximum friction velocity
U_w	wave orbital velocity amplitude at sea bed
$X = \tau_c/(\tau_c + \tau_w)$	relative current strength
$Y = \tau_m/\tau_c + \tau_w)$	dimensionless mean shear stress
$Z = \tau_{max}/\tau_c + \tau_w)$	dimensionless maximum shear stress
z	height above sea bed
z_0	bed roughness length
α	general dimensionless coefficient
δ	wave boundary-layer thickness
ε	eddy viscosity
κ	von Karman's constant $= 0.40$
ν	kinematic viscosity of water
π	$3 \cdot 141592654$
ρ	density of water
τ	horizontal shear-stress in water column
τ_c	current-only bed shear-stress
$\tau_e = \left(\tau_c^2 + \tau_w^2 \right)^{1/2}$	effective bed shear-stress
τ_m	mean bed shear-stress during a wave cycle under combined waves and currents

Notation continued

τ_{max}	maximum bed shear-stress during a wave cycle under combined waves and currents
τ_p	amplitude of oscillatory bed-shear-stress under combined waves and currents
τ_{rms}	root-mean-square bed shear-stress under combined waves and currents
τ_w	amplitude of oscillatory bed shear-stress due to waves
ϕ, ϕ_d	angle between current direction and direction of wave travel in radians, degrees
$\omega = 2\pi / T$	(absolute) radian frequency of waves

Subscripts

c	current-alone
m	mean during wave cycle
max	maximum during wave cycle
rms	root-mean-square over a wave cycle
r	rough-turbulent flow
s	smooth-turbulent flow
w	wave-alone

Contents

Tables

Figures

Contents continued

Appendix

1. Introduction

The main hydrodynamic parameter that controls the erosion, suspension and deposition of muds and sands in estuaries and coastal waters is the *bed shear-stress*, which is the frictional force exerted by the flow per unit area of bed. It is also closely related to the turbulence level of the flow, which controls, for example, suspension of sediments. Methods of calculating the bed shear-stress produced by currents and waves, separately or in combination, are therefore needed. The methods for muddy beds are broadly similar to those used for beds of coarser sediments, but with the difference that the flow is usually assumed to be hydrodynamically smooth for muds whereas it is usually treated as hydrodynamically rough for sands and gravels. The main emphasis in this report is on the less well-researched case of smooth beds, with the overall aim of developing a consistent algorithm applicable to all hydrodynamic states.

In many cases both currents and waves make significant contributions to the bed shear-stress. The resulting bed shear-stress consists of a steady component due to the current together with an oscillatory component due to the waves. If the current and wave velocities over a smooth bed are sufficiently small that the flow remains laminar, then the combined bed shear-stresses are simply a linear addition of the laminar current-alone and wave-alone shear-stresses (see Appendix A). However, in stronger currents and waves the flow will be turbulent, and the turbulence generated in the current and wave boundary layers then adds in a non-linear fashion. Because of this, the mean and oscillatory components of the stress are enhanced beyond the values which would result from a simple linear addition of the steady current-alone stress (τ_c) and the oscillatory wave-alone stress (amplitude τ_w), as shown schematically in Figure 1.

The bed shear-stress $\tau(t)$ varies through a wave cycle in the manner shown schematically by the dotted locus in Figure 1. The most important quantities for use in sediment calculations are:

- the mean value, τ_m, over the wave-cycle
- the maximum value, τ_{max}, during the wave-cycle
- the root-mean-square value, τ_{rms}, taken over the wave-cycle.

The mean, τ_m, is used for determining the friction governing the current, and for determining diffusion of sediment into the outer flow; the maximum, τ_{max}, is used to determine the threshold of sediment motion, and diffusion very near the bed; and τ_{rms} is a good average measure of the shear-stress, particularly useful in random waves. The turbulence generated by the combined current and wave boundary layers causes τ_m to be larger than τ_c, and τ_{max} to be larger than the vector sum of τ_c and τ_w (Figure 1).

More than twenty different theories and models have been proposed to describe the process of Wave-Current Interaction (WCI) over the years, but almost all of them have concentrated on the case of a rough turbulent flow, as would be found over a coarse sand or gravel bed, rather than the smooth turbulent flow commonly found over a freshly deposited mud bed. Some of these theories were discussed and intercompared by Soulsby *et al.* (1993). A parametric fitting method for some of the theories was presented by Soulsby (1997).

Two existing theories that tackle the WCI problem for both rough and smooth beds are those of Myrhaug & Slaattelid (1990) and Antunes do Carmo et al (2003), the latter of which appeared while the present study was in progress.

Most of the existing theoretical predictors involve either an iterative solution, or a full numerical model, which makes their repeated calculation in computational models of the hydrodynamics, sediment dynamics and morphodynamics of estuaries and coastal areas excessively time-consuming. The stresses τ_m, τ_{max} and τ_{rms} should therefore preferably be predicted by explicit algebraic formulae. The method of Carmo et al (2003) was presented in explicit form (fitted to numerical model results), but they only presented comparisons of their theory with measured wave and current stresses separately, not with combined waves and currents.

In previous work an *empirical* explicit formula (DATA2) was devised for rough beds by Soulsby (1995), and for smooth beds a different *empirical* formula was devised for the book by Whitehouse et al (2000). These captured some aspects of the problem, but ignored others. In the present study we seek to derive *physics*-based models for both rough and smooth turbulent flow, while maintaining both simplicity and accuracy.

The tasks required to achieve the study objectives were:

- Devise a new simple-physics explicit rough-bed predictor
- Test this against the empirical DATA2 method
- Adapt the new predictor to the smooth-bed case
- Assemble the existing smooth-bed data
- Implement existing (rough+smooth) predictors: Myrhaug & Slaattelid (1990) and Antunes do Carmo et al (2003)
- Test the new and existing models against smooth-bed data
- Evaluate and compare the performances of the various models.
- Formulate an algorithm to cater for all hydrodynamic states of WCI.

2. Rough beds

We start by considering the case of WCI over a hydrodynamically rough bed. This case is much better researched in terms of both theories and data than the smooth bed case. Ideas that prove to work in the rough-bed case can then be adapted to the smooth-bed case.

2.1 PREVIOUS WORK

A comparison of eight rough-bed WCI models was made in the MAST G6M Coastal Morphodynamics project (Soulsby et al, 1993). These are shown in Figure 2, where the stresses are plotted in a non-dimensional form that emphasises the strength of the non-linearity predicted by the various theories. The data available at that time on mean stresses (τ_m) measured in the field and laboratory by various researchers were also collected together and plotted in the same form, and the model predictions compared with them. The results were published by Soulsby (1995) and summarised by Soulsby (1997).

The different theories differ markedly in their predictions, and in the goodness of their fit to data (Soulsby et al, 1993). The best performing analytical theories were those of Fredsøe (1984) and Grant and Madsen (1979), although both are computationally intensive to use. For simplicity of calculation, a formula known as the DATA2 method was proposed by Soulsby (1995) as a direct fit to 61 laboratory measurements and 70 field measurements of the cycle-mean bed shear-stress τ_m (all for rough beds). The DATA2 formula is:

$$\tau_m = \tau_c \left[1 + 1.2 \left(\frac{\tau_w}{\tau_c + \tau_w} \right)^{3.2} \right] \tag{1}$$

in which τ_c and τ_w are the bed shear-stresses which would occur due to the current alone and to the wave alone, respectively.

The corresponding expression for τ_{max} is given by a vector addition of τ_m from Equation (1) and τ_w.

$$\tau_{max} = \left[\left(\tau_m + \tau_w |\cos\phi| \right)^2 + \left(\tau_w |\sin\phi| \right)^2 \right]^{1/2} \tag{2}$$

where

ϕ = angle between current direction and direction of wave travel.

This is based on an assumption that the enhancement of the oscillatory component of stress caused by the current-induced turbulence is negligible (but note that many of the more sophisticated theories do account for this). Similarly, the root-mean-square bed shear-stress is given by:

$$\tau_{rms} = \left(\tau_m^2 + \frac{1}{2} \tau_w^2 \right)^{1/2} \tag{3}$$

However, the DATA2 formula is based purely on curve-fitting, and it is felt that a more physics-based approach would have a firmer foundation. The aim of the present work was therefore to devise an explicit formula that captures the simplicity and accuracy of the DATA2 method, but has a stronger basis in physics.

2.2 DERIVATION OF NEW THEORY

The first step is to calculate the shear-stresses for current-alone and wave-alone (τ_c and τ_w), which can be predicted by well-established methods. The ones used here are taken from Soulsby (1997, Eqs. 37 and 62). For a current in water of depth h, with density ρ, depth-averaged velocity $\overline{U}$, and bed roughness z_0, the bed shear stress τ_c is given by:

$$\tau_c = \rho C_{Dr} \overline{U}^2 \tag{4}$$

where the subscript "r" denotes rough flow, and

$$C_{Dr} = \left[\frac{0.40}{\ln(h/z_o) - 1} \right]^2 \tag{5}$$

For a sinusoidal wave having period T, and amplitude of the orbital velocity U_w, the amplitude of the bed shear-stress τ_{wr} is given by:

$$\tau_{wr} = \frac{1}{2} \rho f_{wr} U_w^2 \tag{6}$$

where

$$f_{wr} = 1.39(A/z_o)^{-0.52} \tag{7}$$

$$A = U_w T / 2\pi \tag{8}$$

Most of the analytical and computational models of rough-bed (or smooth-bed) WCI make use of an eddy-viscosity assumption, which in general form can be written as:

$$\tau = \rho \varepsilon \frac{\partial U}{\partial z} \tag{9}$$

where τ is the shear-stress, ε is the eddy-viscosity, and U is the velocity at height z. In general, τ, ε and U are functions of z and time. In the most sophisticated models ε varies with both height above the bed and in time throughout the wave-cycle, whereas in simpler models it is constant in time. The latter simplification is adopted here.

It is usual to consider the thin wave boundary layer (wbl), within which intense turbulence is generated in a layer a few centimetres thick above the bed, separately from the outer flow above this. We therefore specify a steady eddy-viscosity profile, inside and outside the wave boundary layer, with a matching current velocity at the interface. It is not strictly necessary for the eddy-viscosity to be continuous at the top of the wbl, and in many theories (e.g. Grant and Madsen, 1979) it is not. We make a valuable simplifying assumption, making use of the experimental finding by Simons et al (2000) that the oscillatory (wave) component of the stress is not enhanced by the current (at

least for wave-dominated combinations). This allows us to specify the eddy-viscosity inside the wbl in terms of only the known quantities τ_c and τ_w, which makes the problem greatly simpler than previous theories, and also explicit. Other theories usually express the eddy-viscosity as a function of the unknown quantities τ_m and τ_{max}, which makes the equations implicit and requires an iterative solution.

The form of eddy-viscosity profile assumed is shown in Figure 3. The general form is similar to that devised by Grant and Madsen (1979), one of the most widely used WCI methods for rough beds. Outside the wbl we assume:

$$\varepsilon = \kappa u_{*m} z (1-z/h) \tag{10}$$

where $u_{*m} = (\tau_m/\rho)^{1/2}$ and $\kappa = 0.40$ is von Karman's constant.

This form ensures that the velocity and shear-stress profiles in this region (i.e. through most of the depth) are consistent with a mean bed shear-stress of τ_m. Inside the wbl we assume

$$\varepsilon = \kappa u_{*e} z \tag{11}$$

where

$$u_{*e} = (\tau_e/\rho)^{1/2} \tag{12}$$

and

$$\tau_e{}^2 = \tau_c{}^2 + \tau_w{}^2 \tag{13}$$

Equation (13) is at the heart of the new method. It states that the "effective shear-stress" τ_e for the purpose of setting the velocity-scale inside the wbl is given (explicitly) by the root-mean-square of the separate current and wave shear stresses. Previous theories have made alternative assumptions about the form of the velocity scale appearing in Eq. (11). The choice of this form is discussed in a later section.

The thickness δ of the wbl is assumed to depend only on the <u>oscillatory</u> part of the velocity, and, furthermore, to depend on the <u>wave-alone</u> friction velocity u_{*w}, as:

$$\delta = a_r \frac{u_{*w}}{\omega} \tag{14}$$

where a_r is a constant to be determined empirically, and $\omega = 2\pi/T$. Similar expressions have been used in previous theories (e.g. Grant & Madsen, 1979), but with the friction velocity including an element of the steady-current shear-stress. The form given by Eq. (14) is preferable because (a) the physical process of formation of the wbl is essentially oscillatory, (b) use of the known quantity u_{*w} makes Eq. (14) explicit.

A lower limit must be set on δ, because the wbl can presumably not be thinner than one grain diameter d of the sediment comprising the bed. Hence the minimum value of δ is taken as $\delta = d$.

Inside the wbl ($0 \leq z \leq \delta$), assuming $\delta \ll h$ and hence $\tau(z) \simeq \rho u_{*m}^2$, Eq. (9) becomes:

$$\rho\varepsilon\frac{dU}{dz} = \rho u_{*m}^2 \tag{15}$$

and using Eq. 11),

$$\kappa u_{*e} z \frac{dU}{dz} = u_{*m}^2 \tag{16}$$

Integrating Eq. (16) w.r.t. z, and applying the boundary condition $U(z_o) = 0$, gives the velocity profile inside the wbl:

$$U(z) = \frac{u_{*m}^2}{\kappa u_{*e}} \ln\left(\frac{z}{z_o}\right) \tag{17}$$

Outside the wbl ($\delta \leq z \leq h$), the shear-stress decreases linearly with height (this follows from time-averaging and vertically-integrating the equation of motion):

$$\tau(z) = \tau_m(1 - \frac{z}{h}) \tag{18}$$

Using Eq. (9) and (10) in (18) gives:

$$\kappa u_{*m} z\left(1 - \frac{z}{h}\right)\frac{dU}{dz} = u_{*m}^2\left(1 - \frac{z}{h}\right) \tag{19}$$

Integrating Eq. (19) w.r.t. z, and applying a matching condition at $z = \delta$ gives:

$$U(z) = U(\delta) + \frac{u_{*m}}{\kappa}\ln\left(\frac{z}{\delta}\right) \tag{20}$$

Making use of Eq. (17) for $U(\delta)$ gives the velocity profile outside the wbl:

$$U(z) = \frac{u_{*m}^2}{\kappa u_{*e}}\ln\left(\frac{\delta}{z_o}\right) + \frac{u_{*m}}{\kappa}\ln\left(\frac{z}{\delta}\right) \tag{21}$$

The depth-averaged velocity $\overline{U}$ is defined by:

$$h\overline{U} = \int_{z_o}^h U(z)dz \tag{22}$$

Substituting Eqs. (17) and (21) into (22) for the ranges $z_o \leq z \leq \delta$ and $\delta < z \leq h$ respectively, and integrating yields:

$$\overline{U} = \frac{u_{*m}^2}{\kappa u_{*e}}\left[\ln\left(\frac{\delta}{z_o}\right) - \frac{\delta}{h} + \frac{z_o}{h}\right] + \frac{u_{*m}}{\kappa}\left[\ln\left(\frac{h}{\delta}\right) - 1 + \frac{\delta}{h}\right] \tag{23}$$

If we make the approximation $z_o \ll \delta \ll h$ (which is valid for most practical cases), then Eq. (23) reduces to (writing $e = \exp(1)$):

$$\overline{U} = \frac{u_{*m}^2}{\kappa u_{*e}} \ln\left(\frac{\delta}{z_o}\right) + \frac{u_{*m}}{\kappa} \ln\left(\frac{h}{e\delta}\right) \tag{24}$$

Equation (24) is a quadratic equation in the unknown u_{*m}, which has the positive solution:

$$u_{*m} = \frac{1}{2a}\left[\left(b^2 + 4a\overline{U}\right)^{1/2} - b\right] \tag{25}$$

where

$$a = \frac{1}{\kappa u_{*e}} \ln\left(\frac{\delta}{z_o}\right) \tag{26}$$

$$b = \frac{1}{\kappa} \ln\left(\frac{h}{e\delta}\right) \tag{27}$$

Both a and b contain only known quantities, so that Eq. (25) is an explicit expression for the mean friction velocity u_{*m}, and hence the mean bed shear-stress $\tau_m = \rho u_{*m}^2$, under combined waves and currents as required. It can alternatively be written in terms of the mean drag coefficient ($C_{Dm} = \tau_m / \rho\overline{U}^2$) as:

$$C_{Dm} = \left[\left(A_1^2 + A_2\right)^{1/2} - A_1\right]^2 \tag{28}$$

where

$$A_1 = \frac{1}{2}\left(\frac{u_{*e}}{\overline{U}}\right) \cdot \frac{\ln(h/\delta) - 1}{\ln(\delta/z_o)} \tag{29}$$

$$A_2 = \frac{\kappa u_{*e}}{\overline{U}} \cdot \frac{1}{\ln(\delta/z_o)} \tag{30}$$

In Eqs (26), (29) and (30) the minimum value of $\delta = d$ must be imposed, as mentioned earlier. For a flat, hydrodynamically rough bed of sediment $z_o = 2.5d/30$. Hence the minimum value of $\delta/z_o = 12$.

The maximum shear-stress τ_{max} is derived by first considering the periodic zero-mean bed shear-stress corresponding to the wave-induced oscillations of the bed shear-stress about the mean value τ_m. A linearising assumption is made such that the periodic stress is written as $\tau_p \sin(\omega t)$. Soulsby (1983, p208) solved this problem of a linearised shear-stress in an oscillatory boundary layer with a steady eddy viscosity increasing linearly with z. The result (Soulsby, 1983, Eq. 35) can be written in terms of the oscillatory wbl in the present problem, within the wbl ($z_o \leq z \leq \delta$) as:

$$\tau_p = \rho u_{*e} U_w \left(\frac{f_{wr}}{2}\right)^{1/2} \tag{31}$$

For strict compatibility the wave friction factor f_w should be obtained from the solution of the oscillatory equation given, for example, by Soulsby (1983, Eq. 36). However, this is a complicated expression in terms of the real and imaginary Kelvin functions (*ker* and *kei*), which would be computationally intensive to calculate. Instead, in order to retain the same level of complexity as in the rest of the derivation, we choose to specify f_w in the simple empirical form of Eq. (7). Then a vector addition of τ_m and τ_p, for waves propagating at an angle of ϕ to the current direction gives:

$$\tau_{max} = \left[\left(\tau_m + \tau_p |\cos \phi| \right)^2 + \left(\tau_p |\sin \phi| \right)^2 \right]^{1/2} \qquad (32)$$

This is a similar expression to that given by Soulsby (1997, Eq. 70) for use with the "DATA2" method for τ_m. It can alternatively be written in terms of the maximum drag coefficient ($C_{Dmax} = \tau_{max} / \rho \overline{U}^2$) as:

$$C_{Dmax} = \left[\left(C_{Dm} + \frac{u_{*e}}{\overline{U}} \cdot \frac{U_w}{\overline{U}} \cdot \left(\frac{f_{wr}}{2} \right)^{1/2} |\cos \phi| \right) + \left(\frac{u_{*e}}{\overline{U}} \cdot \frac{U_w}{\overline{U}} \left(\frac{f_{wr}}{2} \right)^{1/2} |\sin \phi| \right)^2 \right]^{1/2} \qquad (33)$$

where C_{Dm} is calculated from Eq. (28) and all the other quantities are known. The root-mean-square shear-stress is given by:

$$\tau_{rms} = \left(\tau_m^2 + \tfrac{1}{2} \tau_p^2 \right)^{1/2} \qquad (34)$$

It remains to determine the best value for the empirical coefficient a_r (Eq. (14)), based on data. Simons et al (2000, Figure 1), present a semi-logarithmic plot of an experimental velocity profile in combined waves and current. The outer and inner logarithmic fits to the profile (Eqs. 17 and 21) intersect at a height of 18mm. Taking the input parameters of the flows and using Eq. (14) yields a value of $a_r = 0.26$. This is taken as the calibrated value of the coefficient.

Thus explicit expressions for τ_m, τ_{max} and τ_{rms} have been derived for the hydrodynamically rough case, (subject to simplifying assumptions) as given by Eqs. (25), (32) and (34), or in non-dimensional forms by Eqs. (28) and (33). The "recipe" to compute them is given in algorithmic form in Appendix A.

2.3   COMPARISON OF ROUGH-BED METHOD WITH DATA

As an indirect way of testing against data, the new theory was compared with the well-established DATA2 method. The DATA2 method was itself calibrated against a large data-set for mean stresses on rough beds. The comparison is shown in Figure 4, in which the blue and red curves show the new method (mean & max), and the green and purple curves show the corresponding DATA2 method, for inputs of $z_0/h = 1.0 \times 10^{-4}$, $A/z_0 = 1.0 \times 10^{+4}$, $\varphi = 0°$. Further tests were made for other combinations of inputs (Figures 5 and 6). In these, curves are only drawn for combinations of z_o/h and A/z_o that give $A/h \leq 1$, since larger values are not realistic. The new method compares well with the DATA2 method, but the new method is preferred because (a) it has a physical derivation, (b) the results vary with bed-roughness and wave-current angle in a more plausible way. The largest differences occur for τ_{max} under current-dominated conditions, where the new method is up to 20% larger than the DATA2 method. There

is no data that we are aware of to test which method gives the best results, for τ_{max} in this range.

Figure 7 shows the large collection of rough-bed data upon which the DATA2 method was calibrated. It comprises 61 laboratory values and 70 field values of τ_m from 11 published sources listed by Soulsby et al (1993). The data are presented in the same X-Y nondimensionalisation as Figures 4-6. It can be seen that the spread of the data points is broadly similar to the family of curves for the new rough-bed method shown in Figures 4-6.

10

3. Smooth beds

3.1 PREVIOUS WORK

An empirical analytical expression similar to DATA2 was fitted to smooth-bed data and presented in the book Dynamics of Estuarine Muds (Whitehouse et al, 2000). A comprehensive set of laboratory measurements made by Arnskov *et al*. (1993) of bed shear-stresses generated by combined waves and currents over a smooth solid bed gives some indication of the flow behaviour over smooth mud beds (Figure 8). These measurements are described in Section 3.3. Arnskov et al found a significant non-linear enhancement of τ_m for wave-dominated conditions, but no enhancement for current-dominated conditions. Their measurements showed little or no enhancement of τ_{max}, contrary to the predictions of most rough-bed theoretical models. They also found evidence that current-generated turbulence was suppressed by large waves. They tested the rough-bed theoretical model of Fredsøe (1984) against this set of smooth-bed data and found it gave poor agreement. Equation (1) also gives a poor fit to this data. The strangely peaked curve for τ_m is probably a result of the re-laminarisation of the boundary layer in the data of Arnskov et al (1993), discussed in Section 3.3.

Although the general formulation used to derive Equation (1) was based on data for rough beds, it seems reasonable to extend the basic nonlinearity it expresses to the case of smooth beds by fitting its two free coefficients to the data of Arnskov *et al*. (1993). This fitting gave the following equation for smooth beds:

$$\tau_m = \tau_c \left[1 + 9 \left(\frac{\tau_w}{\tau_c + \tau_w} \right)^9 \right] \qquad (35)$$

The values of τ_c and τ_w are calculated using the smooth-turbulent methods given below. The calculations of τ_{max} and τ_{rms} are again given by Equations (2) and (3).

Figure 8 shows that Equation (35) gives a reasonably good fit to the smooth-bed measurements of τ_m and τ_{max} made by Arnskov *et al*. (1993) and Sleath (1990) for waves travelling at 90° to a current. Similar agreement was found for angles of 72° and 108°. This method (Eq. 35) was recommended for use on mud beds by Whitehouse et al (2000), but subsequent evidence suggests that it might not be a general result, because of the laboratory scale effects of the Arnskov et al data (Section 3.3).

3.2 DERIVATION OF NEW THEORY

A similar approach to the new rough-bed theory is developed here for the hydrodynamically smooth case. The friction now depends on the kinematic (molecular) viscosity ν. We replace the bed roughness z_0 with a smooth-turbulent expression:

$$z_0 = \nu/(9u_{*e}) \qquad (36)$$

again with $\tau_e^2 = \tau_c^2 + \tau_w^2$ (Eqs. 12 and 13). This is an adaptation to the WCI case of a widely used expression for steady flows (e.g. see Soulsby, 1997, p. 47). It assumes that a time-invariant value of z_0 can be taken throughout the wave-cycle (rather than varying with $u_*(t)$), consistent with the use of a time-invariant eddy-viscosity assumption. The relevant velocity scale is chosen to be u_{*e}.

To make use of the method we require smooth-turbulent expressions for the current-only drag coefficient C_{Ds} and the wave-only friction factor f_{ws} in terms of current and wave Reynolds numbers (Re_c and Re_w). Various expressions exist for f_{ws} (see Soulsby, 1997, p.79), of which the one used here is (Soulsby, 1997, Eq. 63):

$$f_{ws} = 0.0521 \, Re_w^{-0.187} \quad \text{for } Re_w > 5 \times 10^5 \tag{37}$$

where the subscript "s" denotes smooth flow, and

$$Re_w = U_w A / \nu \tag{38}$$

A new expression was needed to give C_{Ds} explicitly. The smooth-turbulent shear-stress for a steady current is usually calculated iteratively from an implicit equation (see Section 3.2 of Whitehouse et al, 2000). We have approximated this with a fitted explicit expression (accurate to +/-0.7%) as shown in Figure 9:

$$C_{Ds} = 0.0001615 \, \exp[6(Re_c)^{-0.08}] \tag{39}$$

where

$$Re_c = \overline{U}h / \nu \tag{40}$$

This leads to similar explicit expressions for τ_m and τ_{max} for smooth beds to those derived for rough beds. The derivation is analogous to that for the rough-bed case, with the following differences:

In Eqs. (26) and (27), u_{*e}, δ and z_o are given by:

$$u_{*e} = \left(C_{Ds}^2 \overline{U}^4 + \left(\frac{f_{ws}}{2} \right)^2 U_w^4 \right)^{\frac{1}{4}} \tag{41}$$

$$\delta = a_s \frac{u_{*w}}{\omega} \tag{42}$$

$$u_{*w} = \left(\frac{f_{ws}}{2} \right)^{\frac{1}{2}} U_w \tag{43}$$

and z_o given by Eq. (36), C_{Ds} by Eq. (39), and f_{ws} by Eq. (37).

Values of a and b computed in Eqs. (26) and (27) are inserted into Eq. (25) to obtain u_{*m} and hence $\tau_m = \rho u_{*m}^2$. The same substitutions (Eqs. 41-43) can be made in Eqs. (29) and (30) to derive C_{Dm} from Eq. (28), and in Eqs. (31), (32), (33) and (34) to derive τ_p, τ_{max}, C_{Dmax} and τ_{rms} respectively for the smooth-turbulent case.

The coefficient a_s in Eq. (42) is not necessarily assumed equal to a_r for the rough case. Instead, the value of a_s was varied between 0.20 and 0.40 and the percentage of predictions lying within factors 1.1, 1.2, 1.5 and 2 of the Arnskov and Lodahl data were computed (see Section 3.3). The value that gave the best overall agreement with the data was $a_s = 0.22$, which is reasonably close to the rough-bed value $a_r = 0.26$. It was

found that the percentage scores in the optimisation of a_s did not vary strongly for a_s in the range 0.20 to 0.40. Hence a compromise value of $a_r = a_s = 0.24$ has been taken to apply to both rough and smooth cases. This also shows that the general approach is robust, in that the results do not depend critically on the value of the coefficient.

The "recipe" to compute the smooth-turbulent shear-stresses is given in algorithmic form in Appendix A.

3.3   COMPARISON OF SMOOTH-BED METHODS WITH DATA

The new and existing predictors can be compared with smooth-bed wave+current data measured by (a) Arnskov et al (1993) using a flush-mounted hot-film probe on a flat smooth bed in a wave-plus-current basin, and (b) Lodahl et al (1998) in smooth pipes with combined steady and oscillatory flow. Only data from Lodahl's largest diameter pipe (19 cm) has been used in the comparisons described below, as this most nearly approximates to flat-bed conditions. The use of hot-film probes enabled the experimenters to measure both the mean and the maximum bed shear-stresses. Despite the bed not being flat, the Lodahl data is probably more representative of field conditions than the Arnskov data. This is because longer "wave" periods could be used in the pipe than in the basin, so that the wave Reynolds numbers more nearly matched field values. The Arnskov experiments were conducted under laboratory scale conditions, for which the wave-alone conditions were all laminar. The presence of the laminar waves in many cases suppressed the turbulence generation by the current, so that the boundary layer was even less likely to be turbulent than for the corresponding current-alone cases. This re-laminarisation of the flow by the addition of waves has been observed by other laboratory experimenters also. It is not clear to what extent this phenomenon will occur in the field.

The methods of Myrhaug & Slaattelid (1990) [MS90] and Antunes do Carmo et al (2003) [CTS03], were coded up as FORTRAN subroutines. The code for MS90 was the original code written by Olav Slaattelid, and only needed small adaptations for our present purposes. The code for CTS03 was based on the equations referred to in their Table 3. These two existing methods, together with the new method, are compared with the smooth-bed data in Figures 10 to 15.

Figures 10 to 12 show comparisons with the **mean** bed shear stress data (τ_m). The MS90 method (Figure 10) gives good agreement with the Lodahl data at low stresses, but for larger stresses it increases too rapidly with increasing waves. It generally over-estimates the Arnskov data. The CTS03 method (Figure 11) gives good agreement with the Lodahl data for weak waves, but greatly over-estimates the enhancement when stronger waves are added. It also generally over-estimates the Arnskov data. The new method (Figure 12) gives good agreement with the Lodahl data for all combinations of wave and current, but, like the other methods, it over-estimates the Arnskov data.

Figures 13 to 15 show comparisons with the **maximum** bed shear stress data (τ_{max}). The MS90 method (Figure 13) gives good agreement with the Lodahl data for all except the strongest waves, and reasonable agreement with the Arnskov data. The CTS03 method (Figure 14), greatly over-estimates the Lodahl data, but gives good agreement with the Arnskov data. The new method (Figure 15) gives excellent agreement with all the Lodahl data, but somewhat over-estimates the Arnskov data.

The tendency of all the models to over-estimate the Arnskov data is probably due to the re-laminarisation of the laboratory flows, which the models do not reproduce. Greatest

attention should therefore be focussed on the comparisons with the Lodahl data, which is more representative of field conditions.

The three methods have also been tested quantitatively against the Lodahl and Arnskov data-sets, comprising 80 and 45 experimental data-points respectively. For each method, the ratio R of predicted to observed shear-stress was calculated for each data-point, for both τ_m and τ_{max}. The percentage of ratios lying between the range $1/F < R < F$ was calculated for factor $F = 1.1, 1.2, 1.5$ and 2 (Table 1). With only a few exceptions, the percentages lying in each range are largest for the new (Soulsby) method, next for the MS90 method, and thirdly the CTS03 method. This is true for both τ_m and τ_{max}, and the differences are greatest for the most discriminatory ranges of $F = 1.1$ and 1.2. Exceptions are the case of $F = 2$ for τ_{max} where CTS03 scores slightly higher than MS90 which in turn is higher than Soulsby, and $F = 1.5$ for both τ_m and τ_{max}, where MS90 scores slightly higher than Soulsby. It should be mentioned that the coefficient $a_s = 0.22$ in the new method was optimised against the same data-set as the tests in Table 1, but (as mentioned previously) the results are relatively insensitive to the value of a_s, and in fact any value in the range $0.20 \leq a_s \leq 0.40$ would have given broadly the same comparative outcome in Table 1. We therefore conclude that the new method is a significant improvement on the existing models in terms of predicting the mean and maximum bed shear-stresses for smooth beds.

Table 1   Percentage of data-points lying in the range 1/F<R<F where R = predicted/observed shear-stress

For τ_m (mean stresses)				
F =	1.1	1.2	1.5	2
MS90	13.6	24	49.6	75.2
CTS03	10.4	14.4	35.2	67.2
Soulsby	17.6	27.2	48.8	75.2
For τ_{max} (maximum stresses)				
F =	1.1	1.2	1.5	2
MS90	18.4	30.4	56.8	84
CTS03	9.6	20	45.6	84.8
Soulsby	30.4	41.6	55.2	81.6

If only the Lodahl data is used, the performance of the Soulsby method improves to 30, 41, 68 and 75 percent of predictions lying within factors $F=1.1, 1.2, 1.5$ and 2 of the data respectively for τ_m, and 48, 65, 80 and 94 percent for τ_{max}.

4.   Combined method

In general, a flow may be (a) laminar, (b) smooth turbulent, or (c) rough turbulent, with gradual transitions between the three states. The hydrodynamic state of a wave-plus-current flow depends on the current Reynolds number Re_c and the wave Reynolds number Re_w. In order to make a completely general method for calculating WCI bed shear-stresses, an algorithm should be able to cater for all three states and choose the appropriate one. We ignore the gradual transitions in what follows, and simply distinguish between three states of flow.

Lodahl et al (1998) used their measurements to map out the laminar/turbulent boundary as a function of Re_c and Re_w. We have fitted a curve to their data plotting the critical Re_c versus Re_w to derive the following criterion for determining laminar or turbulent WCI flow:

If $Re_c < Re_{c,cr}$ *and* $Re_w < Re_{w,cr}$, then flow is laminar, otherwise it is turbulent

where

$$R_{w,cr} = 1.5 \times 10^5$$
$$Re_{c,cr} = 2000 + (5.92 \times 10^5 \, Re_w)^{0.35}$$

The WCI shear stresses are then calculated as follows. If the flow is laminar, the combined shear-stresses are a simple vector addition of the laminar steady and laminar oscillatory stresses (because the problem is linear). If the flow is turbulent, then both the rough and smooth shear-stresses are calculated by the WCI methods derived in the preceding sections, and the larger value is taken. The rationale for this is that if the roughness elements are fully submerged in the viscous sublayer then the flow will be smooth turbulent, but if the roughness elements protrude through the viscous sublayer then the flow will be rough turbulent and the bed shear-stresses will be larger than for the smooth turbulent case.

The detailed "recipe" is given in algorithmic form in Appendix A.

5. Discussion

The most contentious assumption made to derive the new methods is the form taken for the scale-velocity for the eddy-viscosity inside the wave boundary layer (Eqs. 11 to 13). It might be argued that the use of τ_{max} (or τ_{rms}) instead of τ_e, as used by Grant and Madsen (1979) and others, is more internally consistent. However, we contend that all WCI methods rely on largely hypothetical assumptions, and the pragmatic test of their usefulness is (a) whether they give accurate predictors of the stresses, and (b) whether they are easy to use. Most existing methods tend to over-estimate the strength of the non-linearity, which the present method does not (satisfying criterion (a)), and the use of Eqs. 11 to 13 is what makes the new methods explicit (satisfying criterion (b)).

The choice of Eq. (13) came from considering the more general form:

$$\tau_e^{\,n} = \tau_c^{\,n} + \alpha\tau_w^{\,n} \tag{44}$$

Tests with different values of n showed that n = 2 gave a similar behaviour to the DATA2 method. It also displays a similarity with Eq. (3), and hence τ_e is similar to τ_{rms}. This seems a logical choice since τ_{rms} is a good general-purpose measure of the total turbulence level. However, τ_m in Eq. (3) is replaced by τ_c in Eq. (13), and the factor $\alpha = \frac{1}{2}$ in Eq. (3) is replaced by $\alpha = 1$ in Eq. (13). Values of α other than 1 give rise to an inconsistency, as it is necessary that $\tau_e = \tau_w$ in the case $\tau_c = 0$ to recover the relationship $\tau_{max} = \tau_w$ correctly in the case of waves alone. The use of a time-invariant, vertically-discontinuous eddy-viscosity could also in principle be improved upon, but again this appears to be necessary in order to obtain an explicit solution.

We have assumed in the bulk of this report that muddy beds are hydrodynamically smooth, and sand and gravel beds are hydrodynamically rough. However, strictly it is only a *freshly-deposited* mud bed that is likely to be smooth, and even then it might contain some roughness elements. In certain cases a mud bed may be very rough as a result of trawling activities or bioturbation; for example, box cores of muddy sediments taken at depths of up to 60 m in the Clyde Sea, western Scotland, were found to have had a very disturbed irregular surface with lumps of firm mud several centimetres in height. Bed roughnesses in estuaries may also sometimes be large, for example in areas with a network of fine drainage channels, or as a result of biological activity such as worm-casts. In these cases the *total* bed shear-stress will be governed by the large roughness which incorporates the form-drag created by the pressure field around the roughness elements. Nevertheless, the erosion and deposition of the mud will depend more on the smooth flow over the intervening areas, and the smooth-hydrodynamic equations can be used for this purpose.

For purposes of application in estuarine computational models, it is essential that the bed shear-stresses calculated as inputs to mud erosion/deposition formulae are compatible with those used to derive the threshold bed shear-stress (τ_e and τ_d) and the erosion-rate constant m_e. These site-specific parameters are usually obtained from field or laboratory measurements of mud erosion with author-specific methods of computing the bed shear-stress. Their assumptions about the bed roughness will not always be consistent with those adopted here. Using incompatible values (e.g. rough versus smooth bed values) could lead to unrealistic erosion and deposition rates. Hence values of τ_e, τ_d and m_e should not be taken from the literature uncritically and used with the present methods.

6. Conclusions

- The new predictors for τ_m and τ_{max} for rough beds give broadly similar results to the proven empirical DATA2 method, so they should compare well with data
- Like DATA2, they can be written explicitly (and hence are easy to use) and are robust
- The new predictors for τ_m and τ_{max} for smooth beds are also explicit and robust
- They give better comparisons with smooth-bed data than existing methods, and are simpler
- A general purpose method that caters for laminar, smooth turbulent and rough turbulent flow has been devised and is given in algorithmic form in Appendix A.

7. References

Antunes do Carmo, JS, Temperville, A and Seabra-Santos, FJ (2003). Bottom friction and time-dependent shear-stress for wave-current interaction. J. Hydraulic Res., Vol 41, No.1, 27-37.

Arnskov, MM, Fredsøe, J and Sumer, BM (1993). Bed shear-stress measurements over a smooth bed in three-dimensional wave-current motion. Coastal Engineering, Vol 20, 277-316.

Fredsøe, J (1984). Turbulent boundary layer in wave-current motion. J. Hydraulic Eng. ASCE, Vol 110, 1103-1120.

Grant, WD and Madsen, OS (1979). Combined wave and current interaction with a rough bottom. J. Geophys. Res., Vol 84, No. C4, 1797-1808.

Lodahl, CR, Sumer, BM and Fredsøe, J (1998). Turbulent combined oscillatory flow and current in a pipe. J. Fluid Mech., Vol 373, 313-348.

Myrhaug, D and Slaattelid, OH (1990). A rational approach to wave-current friction coefficients for rough, smooth and transitional turbulent flow. Coastal Engineering, Vol 14, 265-293.

Simons, R, Myrhaug, D, Thais, L, Chapalain, G, Holmedal, L-E and MacIver, R (2000). Bed friction in combined wave-current flows. Coastal Engineering 2000, Proc. 27th Int. Conf., Sydney, Aus, 216-226, ASCE.

Sleath, JFA (1990). Velocities and bed friction in combined flow. In: Proc. 22nd Int. Conf on Coastal Eng., Delft, Vol 1, 450-463, ASCE.

Soulsby, RL (1983). The bottom boundary layer of shelf seas. In: Physical Oceanography of Coastal and Shelf Seas, Ed: B Johns, pp189-266, Elsevier, Amsterdam, ISBN 0-444-42153-X.

Soulsby, RL, Hamm, L, Klopman, G, Myrhaug, D, Simons, RR and Thomas, GP (1993). Wave-current interaction within and outside the bottom boundary layer. Coastal Engineering, Vol (21), 41-69.

Soulsby, RL (1995). Bed shear-stresses due to combined waves and currents. In: Advances in Coastal Morphodynamics, Eds: Stive, MJF, De Vriend, HJ, Fredsøe, J, Hamm, L, Soulsby, RL, Teisson, C and Winterwerp, JC, pp 4-20 to 4-23, Delft Hydraulics, Delft, NL, ISBN 90-9009026-6.

Soulsby, RL (1997). Dynamics of Marine Sands: a manual for practical applications. Thomas Telford, London, ISBN 0-7277-2584-X.

Whitehouse, RJS, Soulsby, RL, Roberts, W and Mitchener, HJ (2000). Dynamics of Estuarine Muds: a manual for practical applications. Thomas Telford, London, ISBN 0-7277-2864-4.
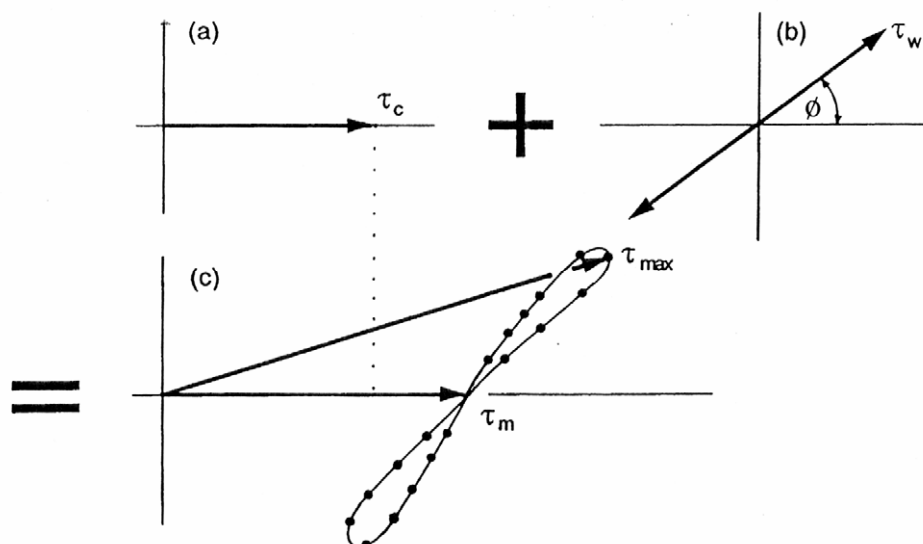
Figures

Figure 1. **Schematic diagram of non-linear interaction of wave and current bed shear-stress (re-printed from Soulsby et al. (1993), Coastal Engineering. 21, 41-69, by permission of Elsevier Science Publisher, BV)**
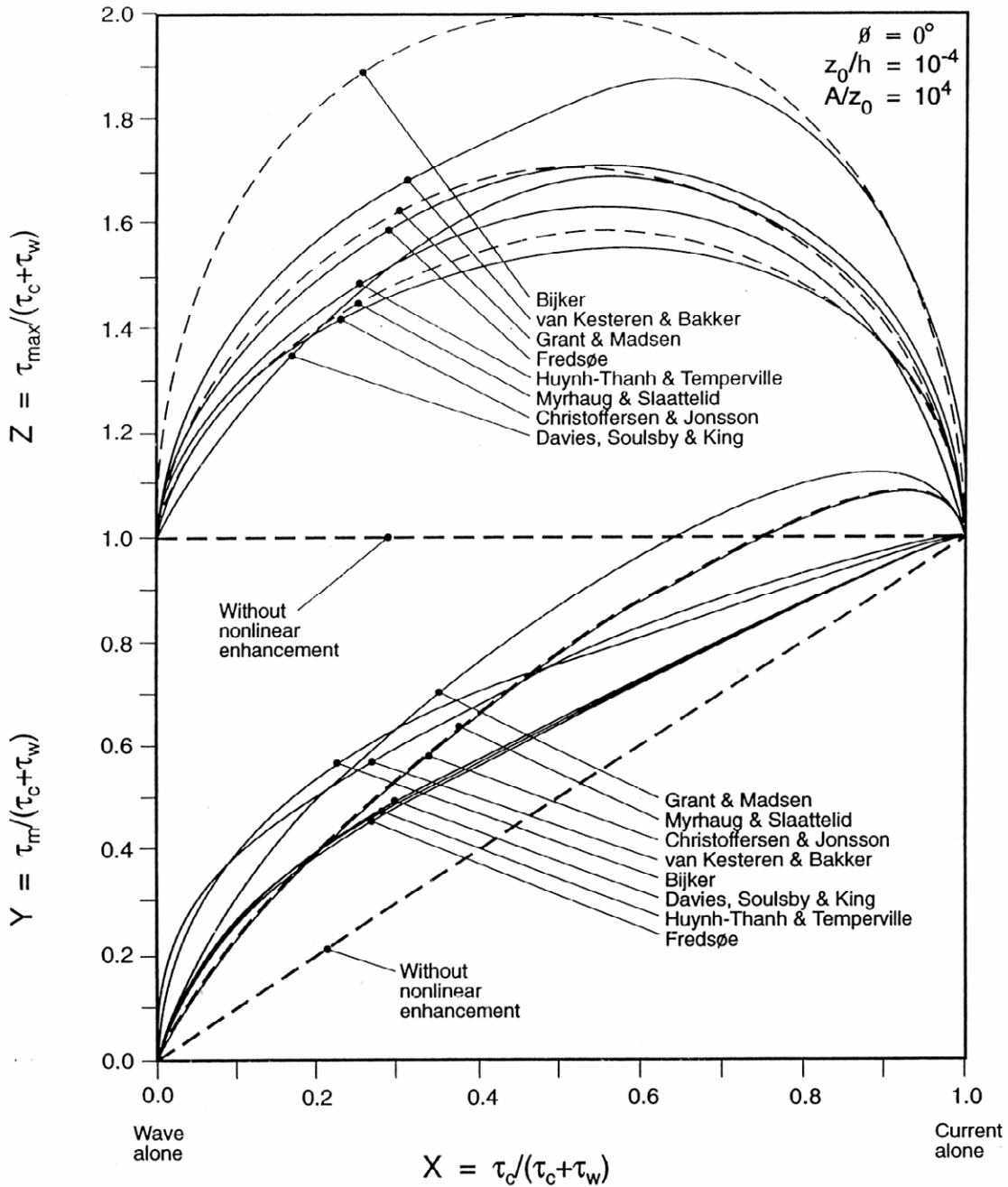
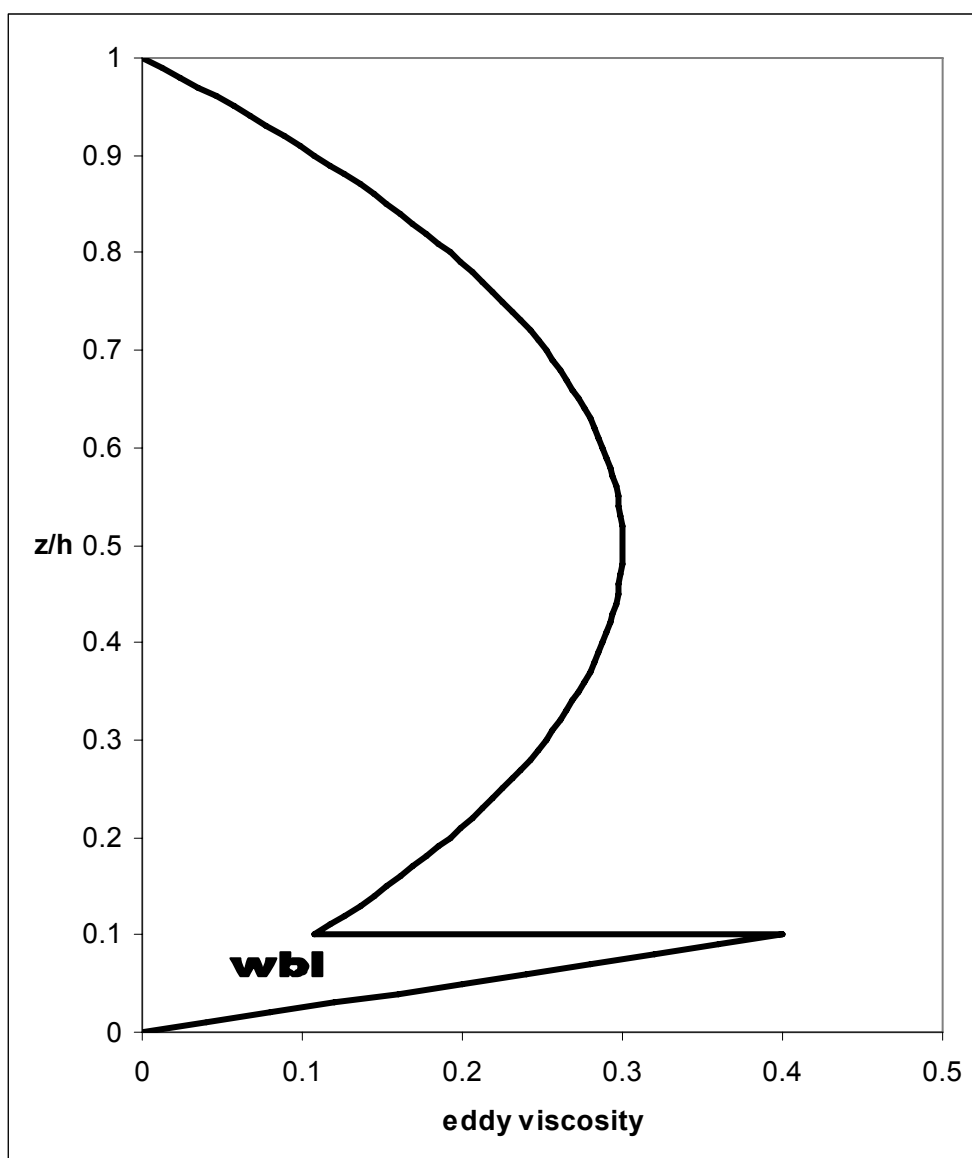**Figure 2.** *Intercomparison of eight models for prediction of mean (τ_m) and maximum (τ_{max}) bed shear-stress due to waves plus a current (reprinted from Soulsby et al. (1993), Coastal Engineering, 21, 41-69, by permission of Elsevier Science Publishers, BV)*

Figure 3. *Schematic diagram of eddy-viscosity profile adopted for the new rough and smooth WCI models*
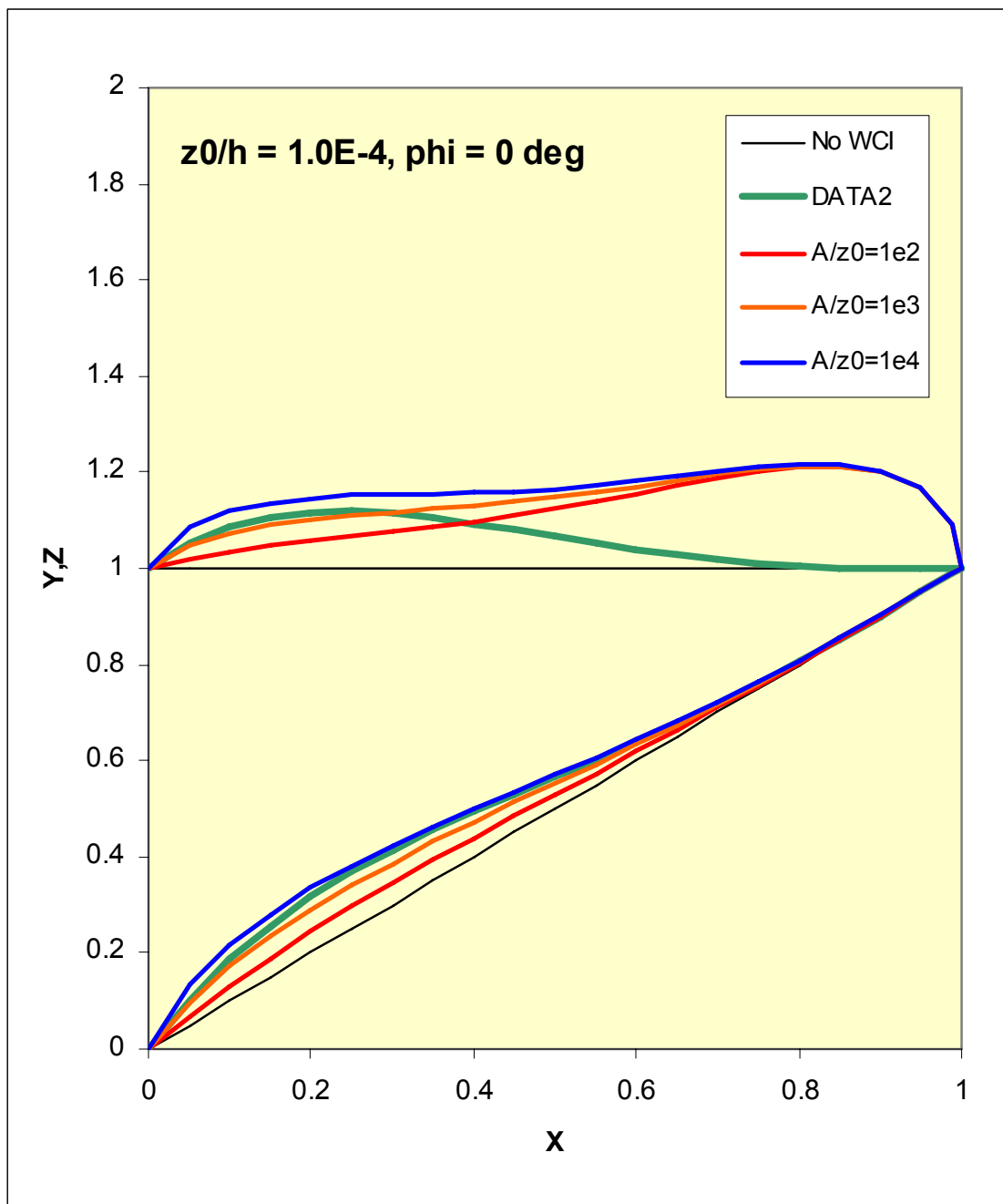
Figure 4. *Comparison of new rough-bed model with the DATA2 model for input values shown. X, Y and Z defined in Figure 2*
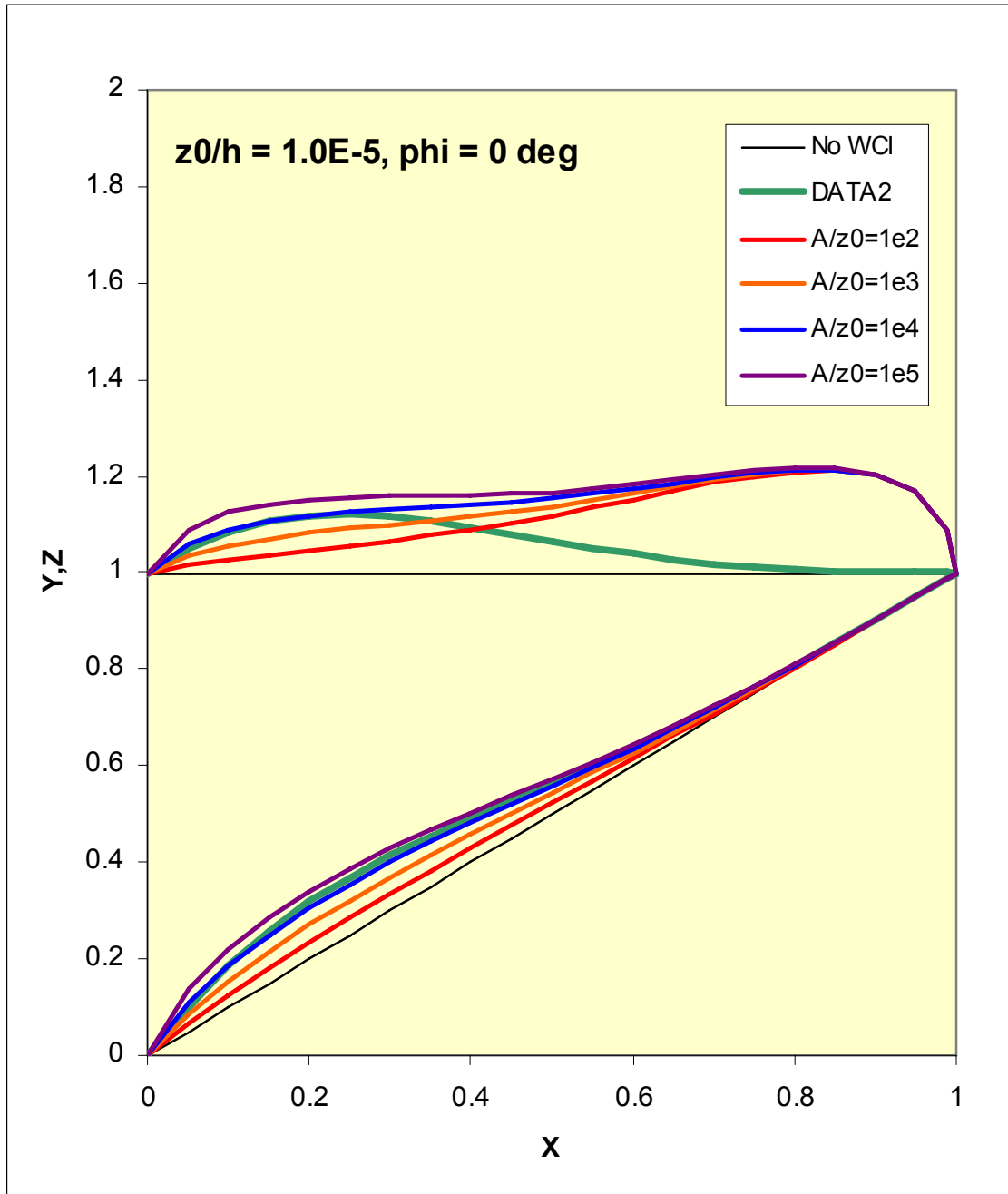
Figure 5. Comparison of new rough-bed model with the DATA2 model for input values shown
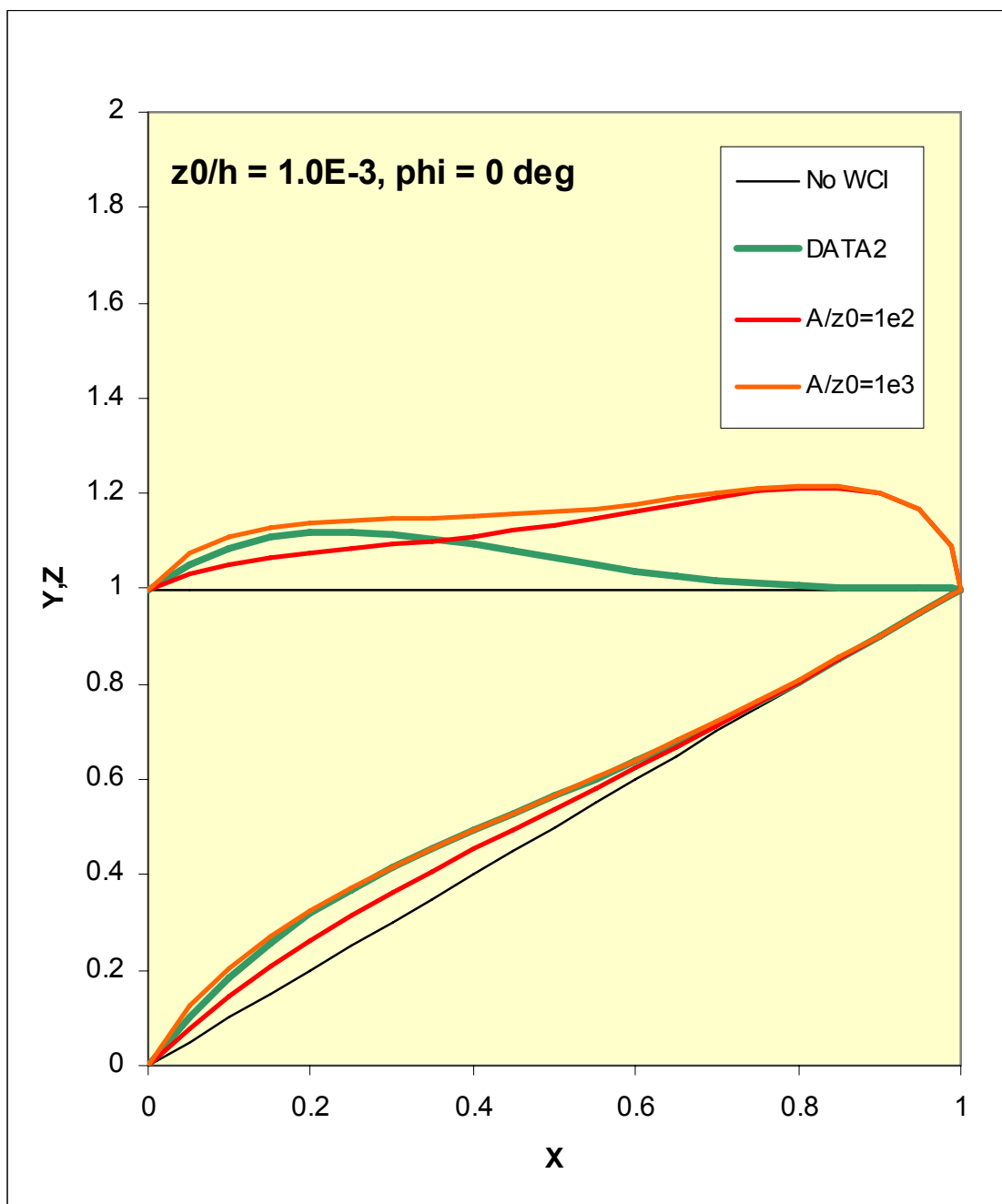
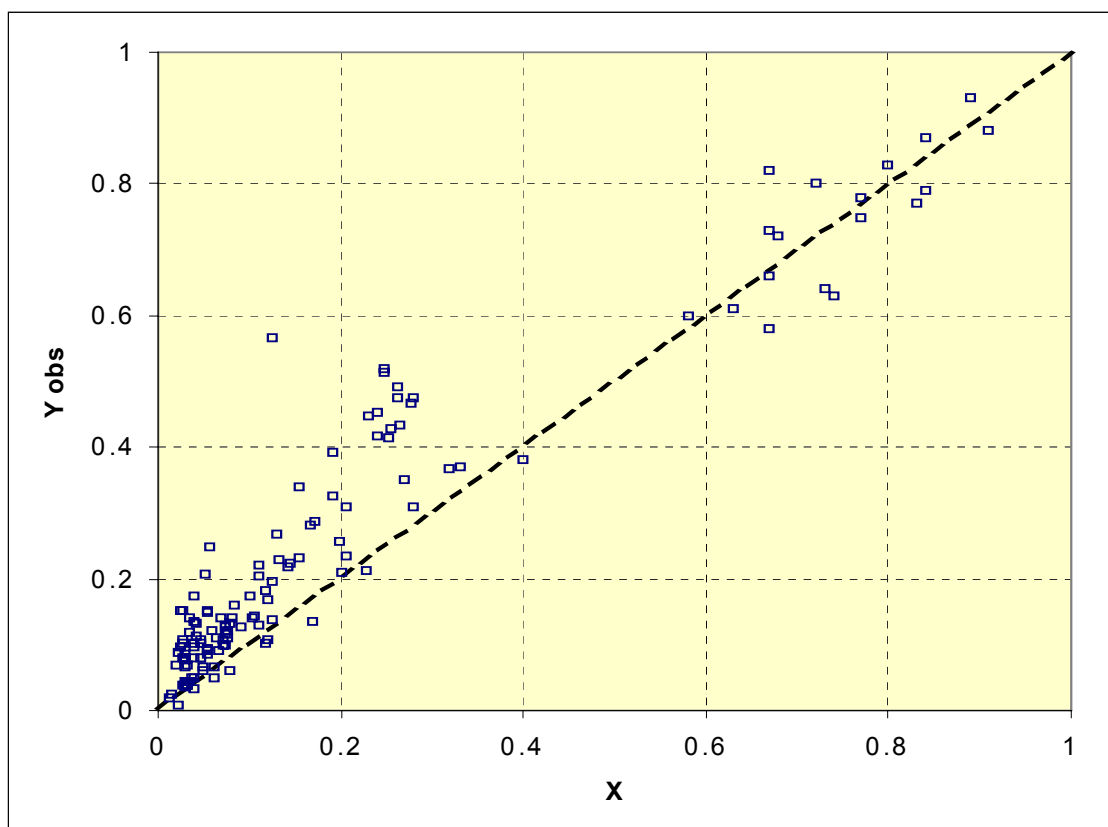**Figure 6. Comparison of new rough-bed model with the DATA2 model for input values shown**

Figure 7. *Data for τ_m from laboratory and field measurements by authors listed by Soulsby et al (1993). X and Y defined in Figure 2*
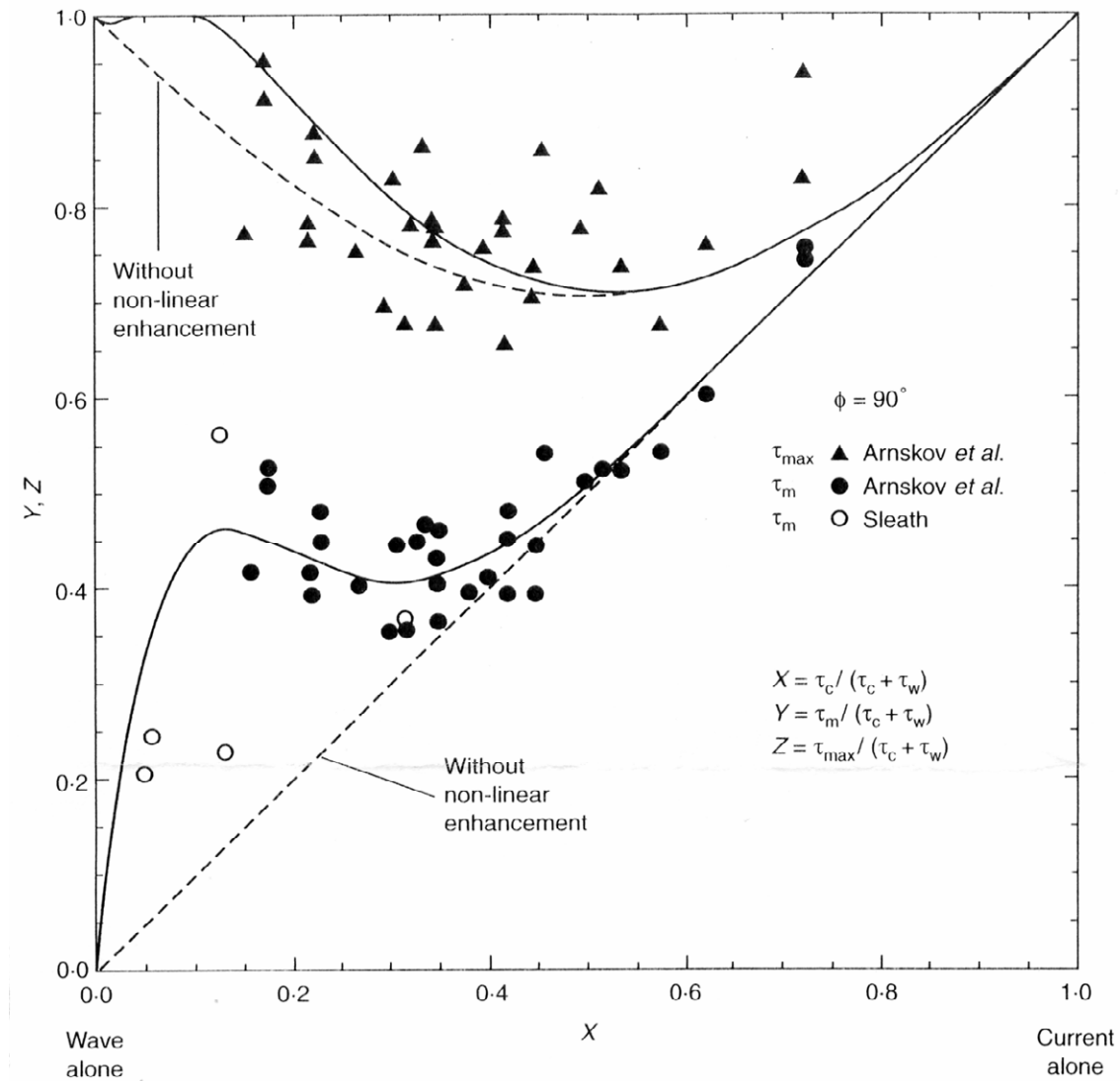
Figure 8. *Comparison of fitted curves with data for the mean τ_m and maximum τ_{max} values of the wave current shear-stress; waves and currents crossing at right angles (Whitehouse et al, 2000). Data from Arnskov et al. (1993) and Sleath (1990). X, Y and Z defined in Figure 2*
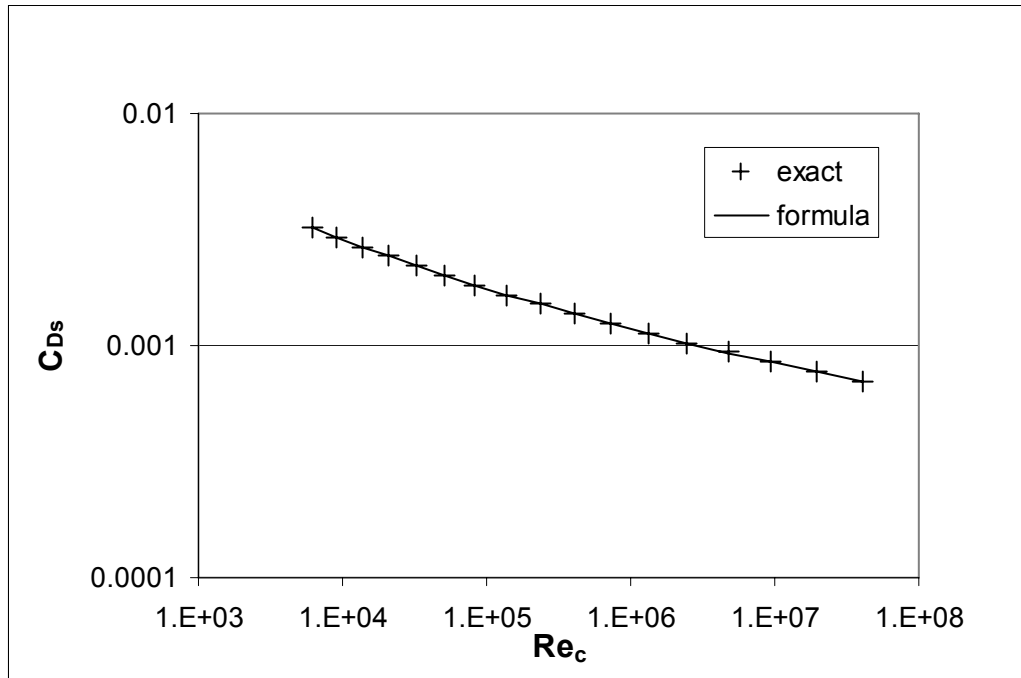
Figure 9. **Comparison of fitted formula for smooth drag coefficient C_{DS} (curve) with full solution (symbols)**
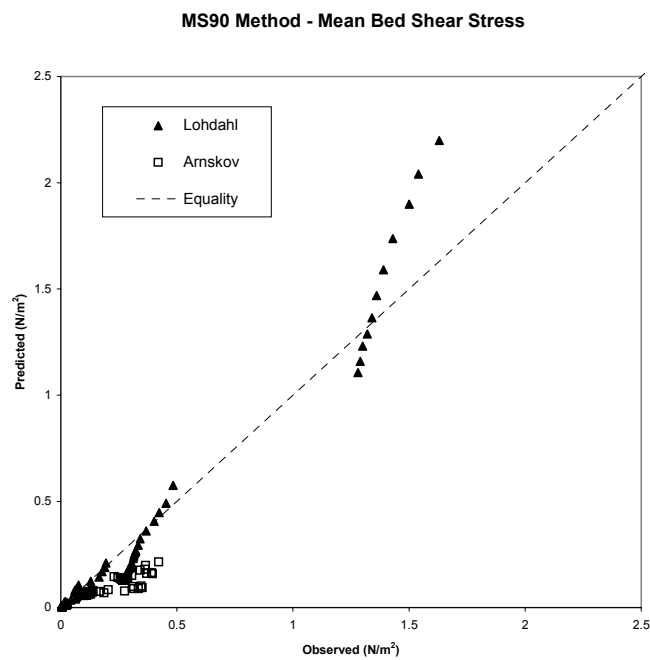

Figure 10. **Comparison of mean shear-stress predictions by MS90 method with smooth-bed data**
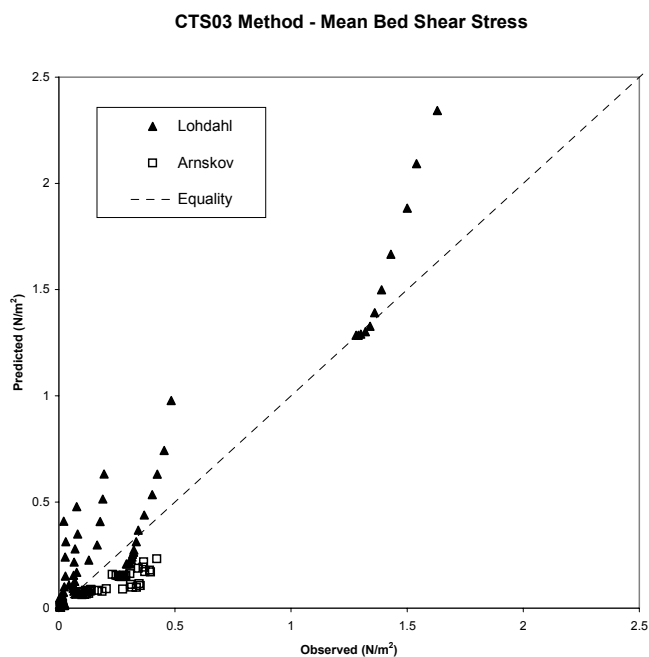
Figure 11. Comparison of mean shear-stress predictions by CTS03 method with smooth-bed data
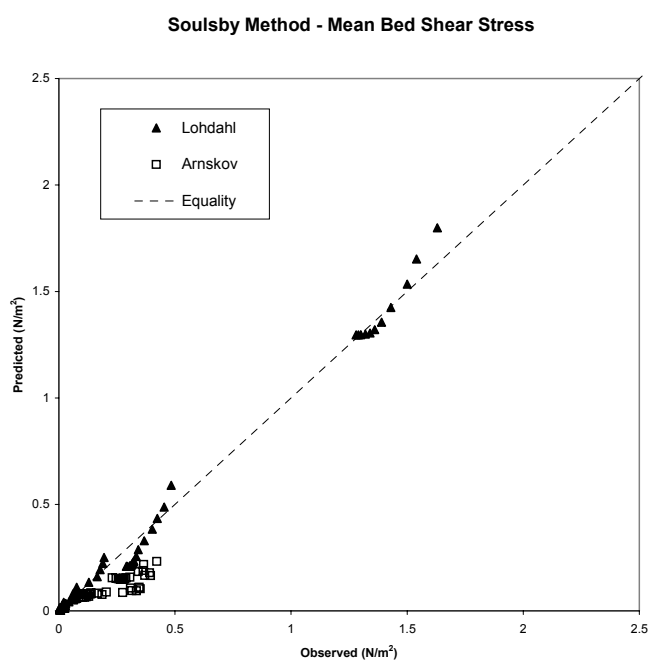
Figure 12. Comparison of mean shear-stress predictions by Soulsby method with smooth-bed data

MS90 Method - Maximum Bed Shear Stress
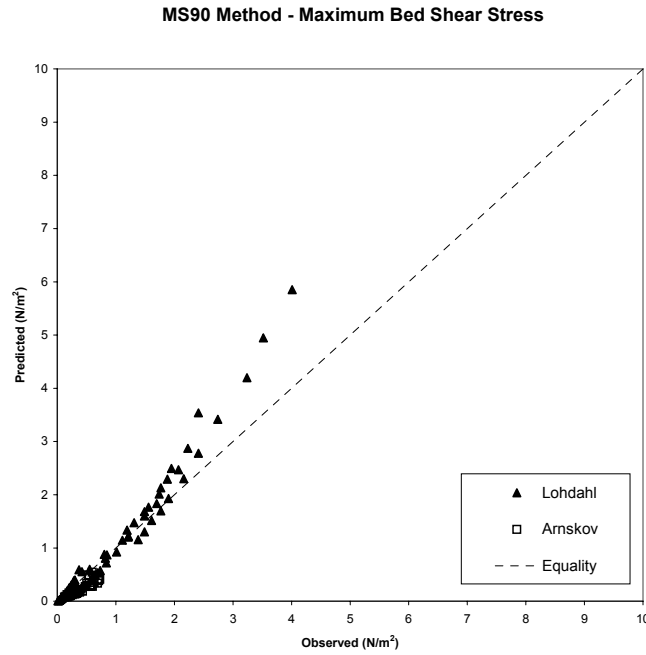
Figure 13. Comparison of maximum shear-stress predictions by MS90 method with smooth-bed data

CTS03 Method - Maximum Bed Shear Stress
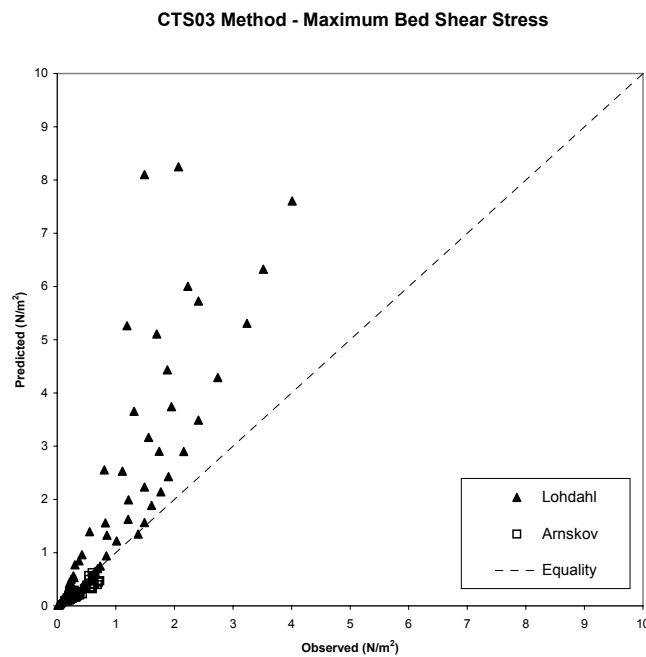
Figure 14. Comparison of maximum shear-stress predictions by CTS03 method with smooth-bed data

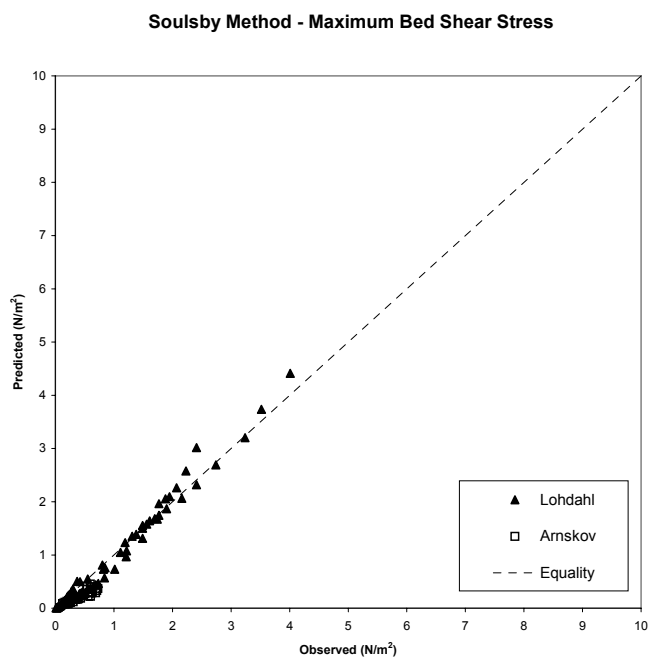**Soulsby Method - Maximum Bed Shear Stress**

Figure 15. Comparison of maximum shear-stress predictions by Soulsby method with smooth-bed data

Appendix

Appendix A Algorithm for calculating mean, maximum and r.m.s. bed shear-stresses for laminar, smooth-turbulent and rough-turbulent wave-plus-current flows

A.1   Inputs

Water depth (m)	h	
Water density (kgm^{-3})	ρ	
Kinematic viscosity ($m^2\,s^{-1}$)	ν	
Median grain diameter of bed (m)	d_{50}	(= 0 for smooth bed)
Wave orbital velocity amplitude (ms^{-1})	U_w	
Wave period (s)	T	
Depth-averaged current speed (ms^{-1})	$\overline{U}$	
Angle between wave and current directions (degrees)	ϕ_d	($0° \leq \phi_d \leq 360°$)
Acceleration due to gravity (ms^{-2})	g	($9.81ms^{-2}$)

A.2   Outputs

Current-alone bed shear-stress (Nm^{-2})	τ_c
Wave-alone bed shear-stress amplitude (Nm^{-2})	τ_w
Mean wave-plus-current bed shear-stress (Nm^{-2})	τ_m
Maximum wave-plus-current bed shear-stress (Nm^{-2})	τ_{max}
Root-mean-square wave-plus-current bed shear-stress (Nm^{-2})	τ_{rms}

A.3   Calculate basic parameters

Convert ϕ_d to radians $\qquad \phi = \phi_d \, \pi/180$
Convert d_{50} to bed roughness length (rough flow) $\qquad z_o = d_{50}/12$

Calculate current Reynolds Number

$$Re_c = \frac{\overline{U}h}{\nu} \tag{A1}$$

Calculate wave semi-orbital excursion

$$A = \frac{U_w T}{2\pi} \tag{A2}$$

Calculate wave Reynolds Number

$$Re_w = \frac{U_w A}{\nu} \tag{A3}$$

Calculate drag coefficient for current for smooth turbulent flow
$$C_{Ds} = 0.0001615 \, \exp\left[6(Re_c)^{-0.08}\right] \tag{A4}$$

Calculate wave friction factor for smooth turbulent flow
$$f_{ws} = 0.0521 \, Re_w^{-0.187} \tag{A5}$$

Calculate drag coefficient for current for rough turbulent flow

$$C_{Dr} = \left[\frac{0.40}{\ln(h/z_o) - 1}\right]^2 \tag{A6}$$

Calculate wave friction factor for rough turbulent flow

$$f_{wr} = 1.39 \left(\frac{A}{z_o} \right)^{-0.52} \tag{A7}$$

A.4   Determine flow regime

A.4.1   If $\overline{U} = 0$ and $U_w = 0$, then no flow

$$\tau_m = \tau_{max} = 0 \tag{A8}$$

A.4.2   If $\overline{U} > 0$ and $U_w = 0$, then current-only flow
If $Re_c \leq 2000$, then laminar flow

$$\tau_m = \tau_{max} = \frac{3\rho v \overline{U}}{h} \tag{A9}$$

If $Re_c > 2000$, then turbulent flow

Calculate $\tau_{mr} = \rho C_{Dr} \overline{U}^2$ (rough) $\tag{A10a}$

and $\tau_{ms} = \rho C_{Ds} \overline{U}^2$ (smooth) $\tag{A10b}$

then $\tau_m = \tau_{max} = \max(\tau_{mr}, \tau_{ms})$ $\tag{A11}$

A.4.3   If $\overline{U} = 0$ and $U_w > 0$, then wave-only flow
If $Re_w \leq 1.5 \times 10^5$, then laminar flow

$$\tau_m = 0, \tau_{max} = \rho Re_w^{-0.5} U_w^2 \tag{A12}$$

If $Re_w > 1.5 \times 10^5$, then turbulent flow

Calculate $\tau_{wr} = \frac{1}{2}\rho f_{wr} U_w^2$ (f_{wr} from Eq. (A7)) $\tag{A13}$

and $\tau_{ws} = \frac{1}{2}\rho f_{ws} U_w^2$ (f_{ws} from Eq. (A5)) $\tag{A14}$

then $\tau_m = 0, \tau_{max} = \max(\tau_{wr}, \tau_{ws})$ $\tag{A15}$

A.4.4   If $\overline{U} > 0$ and $U_w > 0$, then combined wave and current flow
Calculate critical current Reynolds number
$Re_{c,cr} = 2000 + (5.92 \times 10^5 \times Re_w)^{0.35}$ $\tag{A16}$
$Re_{w,cr} = 1.5 \times 10^5$
If $Re_c \leq Re_{c,cr}$ *and* $Re_w \leq Re_{w,cr}$, then laminar flow
τ_m given by Eq. (A9)

$$\tau_w = \rho Re_w^{-0.5} U_w^2 \tag{A17}$$

$$\tau_{max} = \left[\left(\tau_m + \tau_w |\cos \phi| \right)^2 + \left(\tau_w |\sin \phi| \right)^2 \right]^{\frac{1}{2}} \tag{A18}$$

If $Re_c > Re_{c,cr}$ *or* $Re_w > Re_{w,cr}$, then turbulent flow
Calculate $\tau_{m,r}$ and $\tau_{max,r}$ for rough flows using method given in Section A.5
Calculate $\tau_{m,s}$ and $\tau_{max,s}$ for smooth flows using method given in Section A.6
If $\tau_{max,r} > \tau_{max,s}$, then flow is rough turbulent

$\tau_m = \tau_{m,r}$, $\tau_{max} = \tau_{max,r}$ $\tag{A19a}$

If $\tau_{max,r} \leq \tau_{max,s}$, then flow is smooth turbulent

$\tau_m = \tau_{m,s}$, $\tau_{max} = \tau_{max,s}$ $\tag{A19b}$

The values of τ_c and τ_w must be calculated for the flow regime determined above, namely Eqs. (A9) and (A12) for laminar flow, Eqs. (A10a) and (A13) for rough turbulent flow, and Eqs. (A10b) and (A14) for smooth turbulent flow.

A.5 Rough-turbulent wave-plus-current shear-stresses

Set $a_r = 0.24$

Calculate
$$T_1 = \frac{\delta}{z_o} = \max \left\{ a_r \left(\frac{f_{wr}}{2} \right)^{1/2} \left(\frac{A}{z_o} \right), 12 \right\} \tag{A20}$$

with f_{wr} from Eq. (A7)
$$T_2 = \frac{h}{\delta} = \frac{h}{T_1 z_o} \tag{A21}$$

$$T_3 = \frac{u_{*e}}{\overline{U}} = \left[C_{Dr}^2 + \left(\frac{f_{wr}}{2} \right)^2 \left(\frac{U_w}{\overline{U}} \right)^4 \right]^{1/4} \tag{A22}$$

with C_{Dr} from Eq. (A6)
$$A_1 = \frac{T_3 \left[\ln(T_2) - 1 \right]}{2 \ln(T_1)} \tag{A23}$$

$$A_2 = \frac{0.40\, T_3}{\ln(T_1)} \tag{A24}$$

$$C_{Dm} = \left[\left(A_1^2 + A_2 \right)^{1/2} - A_1 \right]^2 \tag{A25}$$

$$C_{Dmax} = \left[\left(C_{Dm} + T_3 \cdot \frac{U_w}{\overline{U}} \cdot \left(\frac{f_{wr}}{2} \right)^{1/2} \cdot |\cos \phi| \right)^2 + \left(T_3 \frac{U_w}{\overline{U}} \left(\frac{f_{wr}}{2} \right)^{1/2} \cdot |\sin \phi| \right)^2 \right]^{1/2} \tag{A26}$$

$$\tau_m = \rho\, C_{Dm}\, \overline{U}^2 \tag{A27}$$
$$\tau_{max} = \rho\, C_{Dmax}\, \overline{U}^2 \tag{A28}$$

A.6 Smooth turbulent wave-plus-current shear-stress

Set $a_s = 0.24$
Calculate

$$T_1 = 9\, a_s\, Re_w \left(\frac{f_{ws}}{2} \right)^{1/2} \left[C_{Ds}^2 \left(\frac{\overline{U}}{U_w} \right)^4 + \left(\frac{f_{ws}}{2} \right)^2 \right]^{1/4} \tag{A29}$$

with f_{ws} from Eq. (A5), C_{Ds} from Eq. (A4)
$$T_2 = \left(\frac{Re_c}{Re_w} \right) \cdot \left(\frac{U_w}{\overline{U}} \right) \cdot \frac{1}{a_s} \cdot \left(\frac{2}{f_{ws}} \right)^{1/2} \tag{A30}$$

$$T_3 = \left[C_{Ds}^2 + \left(\frac{f_{ws}}{2} \right)^2 \cdot \left(\frac{U_w}{\overline{U}} \right)^4 \right]^{1/4} \tag{A31}$$

Calculate A_1 from Eq. (A23), A_2 from Eq. (A24), C_{Dm} from Eq. (A25), C_{Dmax} from Eq. (A26) <u>except</u> replace f_{wr} with f_{ws}, τ_m from Eq. (A27), τ_{max} from Eq. (A25)

A.7 RMS shear-stress for waves plus current

Calculate τ_m using the methods given above appropriate to laminar, smooth-turbulent or rough-turbulent flow regime.

Calculate τ_w from Eq. (A17) if flow is laminar, or Eqs. (A5) and (A14) if flow is smooth turbulent, or Eqs. (A7) and (A13) if flow is rough turbulent. The flow regime is determined by the criteria given in Section A.4.4.

Calculate root-mean-square shear-stress

$$\tau_{rms} = \left(\tau_m^2 + \tfrac{1}{2}\tau_w^2 \right)^{\frac{1}{2}} \tag{A32}$$

A.8 Worked examples

The following inputs and outputs are provided so that users can check they get the same answers. The full step-by-step working is not given, since it would be rather lengthy.

A.8.1 Laminar flow

Inputs: $h = 0.1m$, $\rho = 1000 kgm^{-3}$, $\nu = 1.0 \times 10^{-6} m^2 s^{-1}$, $d_{50} = 0$ (smooth bed), $U_w = 0.2 ms^{-1}$, $T = 10s$, $\overline{U} = 0.06 ms^{-1}$, $\phi_d = 0^0$

Outputs: $(\tau_c, \tau_w, \tau_m, \tau_{max}, \tau_{rms}) = (0.0018, 0.1585, 0.0018, 0.1603, 0.1121)\ Nm^{-2}$

A.8.2 Smooth turbulent flow

Inputs: $h = 0.4m$, $\rho = 1000 kgm^{-3}$, $\nu = 1.0 \times 10^{-6} m^2 s^{-1}$, $d_{50} = 0$ (smooth bed), $U_w = 0.4 ms^{-1}$, $T = 2s$, $\overline{U} = 0.3 ms^{-1}$, $\phi_d = 75^0$

Outputs: $(\tau_c, \tau_w, \tau_m, \tau_{max}, \tau_{rms}) = (0.1530, 0.5492, 0.2194, 0.6518, 0.4460)\ Nm^{-2}$

A.8.3 Rough turbulent flow

Inputs: $h = 5m$, $\rho = 1000 kgm^{-3}$, $\nu = 1.0 \times 10^{-6} m^2 s^{-1}$, $d_{50} = 0.001m$, $U_w = 0.7 ms^{-1}$, $T = 8s$, $\overline{U} = 0.5 ms^{-1}$, $\phi_d = 90^0$

Outputs: $(\tau_c, \tau_w, \tau_m, \tau_{max}, \tau_{rms}) = (0.3998, 2.7353, 0.7236, 2.8434, 2.0651)\ Nm^{-2}$